


Ultrasound-Targeted Microbubble Destruction-Mediated miR-206 Overexpression Promotes Apoptosis and Inhibits Metastasis of Hepatocellular Carcinoma Cells Via Targeting PPIB

Technology in Cancer Research & Treatment
Volume 19: 1-11
© The Author(s) 2020
Article reuse guidelines:
sagepub.com/journals-permissions
DOI: 10.1177/1533033820959355
journals.sagepub.com/home/tct


Huating Wu, BSc¹, Dawei Xie, BSc², Yingxia Yang, BSc¹, Qing Yang, BSc¹, Xiajun Shi, BSc¹, and Rong Yang, BSc¹ 

Abstract

Background: Ultrasound-targeted microbubble destruction (UTMD) has been found to be an effective method for delivering microRNAs (miRNAs, miRs). The current study is aimed at discovering the potential anti-cancer effects of UTMD-mediated miR-206 on HCC. **Methods:** In our study, the expressions of miR-206 and peptidyl-prolyl *cis-trans* isomerase B (PPIB) in HCC tissues and cells were detected by quantitative real-time polymerase chain reaction (qRT-PCR). PPIB expressions in HCC and adjacent normal tissues were analyzed by gene expression profiling interactive analysis (GEPIA). MiR-206 mimic and mimic control were transfected into HCC cells using UTMD. Potential binding sites between miR-206 and PPIB were predicted and confirmed by TargetScan and dual-luciferase reporter assay, respectively. Cell migration, invasion, and apoptosis were detected by wound healing assay, Transwell, and flow cytometry, respectively. The expressions of apoptosis-related proteins (Bax, Bcl-2), Epithelial-to-mesenchymal (EMT) markers (E-cadherin, N-cadherin and Snail) and PPIB were measured by Western blot. **Results:** MiR-206 expression was downregulated while PPIB expression was upregulated in HCC, and PPIB was recognized as a target gene of miR-206 in HCC tissues. UTMD-mediated miR-206 inhibited HCC cell migration and invasion while promoting apoptosis via regulating the expressions of proteins related to apoptosis, migration, and invasion by targeting PPIB. **Conclusion:** Our results suggested that the delivery of UTMD-mediated miR-206 could be a potential therapeutic method for HCC treatment, given its effects on inhibiting cell migration and invasion and promoting cell apoptosis.

Keywords

ultrasound-targeted microbubble destruction (UTMD), miR-206, hepatocellular carcinoma, peptidyl-prolyl *cis-trans* isomerase B (PPIB), apoptosis, metastasis

Abbreviations

UTMD, ultrasound-targeted microbubble destruction; PPIB, peptidyl-prolyl *cis-trans* isomerase B; qRT-PCR, quantitative real-time polymerase chain reaction; GEPIA, gene expression profiling interactive analysis; EMT, epithelial-to-mesenchymal; HCC, hepatocellular carcinoma; miRNAs, microRNAs; 3'-UTR, 3'-untranslated region; mRNAs, message RNAs; CDK9, cyclin-dependent kinase 9; PVDF, polyvinylidene fluoride; BCA, bicinchoninic acid; HRP, horseradish peroxidase; TBST, tris-buffer saline tween; ECL, enhanced chemiluminescence; PI, propidium iodide; PBS, phosphate buffered saline; SD, standard deviation

Received: February 25, 2020; Revised: August 13, 2020; Accepted: August 21, 2020.

¹ Department of Ultrasound, Dingxi People's Hospital, Dingxi, Gansu Province, China

² Department of General Surgery, Dingxi People's Hospital, Dingxi, Gansu Province, China

Corresponding Author:

Rong Yang, Department of Ultrasound, Dingxi People's Hospital, No.22, Ding'an Road, Ding'an District, Dingxi, Gansu Province 743000, China.
Email: yaro_yarong@163.com



Introduction

Hepatocellular carcinoma (HCC) is a highly angiogenic solid tumor molecularly characterized by cell cycle dysfunction, angiogenesis aberrance and apoptosis evasion.¹ As the most common type of primary liver cancer in adults, HCC has been recognized as the leading cause of cancer-related death around the world,² which thus represents a major health problem.³ Therefore, it is of great urgency and significance to find a potential therapeutic method for HCC treatment.

MicroRNAs (miRNAs) have been widely used as biomarkers to promote tumor genesis identification and characterization in a variety of studies.⁴ The miRNA family comprises highly conserved small ncRNAs with a length of 19-25 nucleotides and the ability to regulate gene expression through combining with 3'-untranslated regions (3'-UTRs) of target message RNAs (mRNAs).⁵ Dysregulation of miRNAs has been found in multiple human malignancies, such as HCC cells.⁶ For example, miR-206 has been found to inhibit HCC cell growth via targeting cyclin-dependent kinase 9 (CDK9).⁷ However, there is a lack of studies on its relation with peptidyl-prolyl *cis-trans* isomerase B (PPIB) in HCC cells.

PPIB (cyclophilin B, CypB), a member of the PPIase family, has been found to contribute to protein folding.⁸ In cancer biology, as Choi et al. pointed out, PPIB is related to malignant progression and regulation of genes.⁹ As for HCC, Kim et al. revealed that hypoxia-induced PPIB can stimulate HCC cell survival via a positive feedback loop with hypoxia-inducible factor-1 α (HIF-1 α).¹⁰ However, its relation with miR-206 in HCC cells is rarely discussed.

Recently, microbubble ultrasound contrast agent has emerged as a novel safe and stable vector for gene transfer, where genes of interest contained in microbubbles were released the moment the microbubbles were broken.¹¹ Vibration-induced destruction of microbubbles has been found to facilitate the irreversible process of local cell permeability increase and soundhole production, thereby promoting genes to enter into the nucleus and increasing their expressions and transfection efficiency.¹² In addition, microbubbles could efficiently transport genes or drugs by avoiding degradation caused by blood endonucleases or other lytic enzymes.^{13,14} Viral vector has been used as a highly efficient method for gene delivery to a variety of tissues, but its clinical application is limited due to the risk of specific immune responses.¹⁵ By contrast, ultrasound-targeted microbubble destruction (UTMD), a non-viral technique, is able to easily deliver genes and drugs to targeted tissues or organs through blood circulatory system¹¹ with a low risk of adverse systemic responses.¹⁶ Moreover, UTMD allows for site-specific drug and gene delivery *in vitro* and *in vivo* via a process called sonoporation.^{17,18} Therefore, it has been proposed that this microbubble-based technique may help ameliorate gene transfection efficiency and is likely to be used as a brand-new therapeutic method for treating cancer.¹⁹

Based on the potential role of miR-206 played in HCC progression and development,⁷ the present study aimed to

assess the transfection efficiency and safety of UTMD-mediated miR-206 in human HCC HepG2 cells, and investigate the role of miR-206 in HCC development and progression as well as the feasibility of UTMD-mediated gene therapy.

Materials and Methods

Ethics Statement

Approval of the study was obtained from the ethics committee of Dingxi People's Hospital (approval number: ZLK20181003) and all patients gave written informed consent.

Sample Collection

In this study, clinical samples of HCC tissues (n = 42) and paired normal adjacent tissues (n = 42) of patients were collected from Dingxi People's Hospital between 2018 October and 2019 May. Adjacent tissues were obtained at approximately 5 cm from HCC tissues. The patients conformed to the following criteria: a) no history of chemotherapy or radiotherapy; b) without other cancers, autoimmune diseases, contagious diseases, etc. All clinical samples were available at the time of initial resection and preserved at -80°C refrigerator after phosphate buffer saline (PBS) washing.

Cell Culture

Human HCC HepG2 cells (catalog number: HB-8065) were bought from the American type culture collection (ATCC; Rockville, MD, USA; <https://www.atcc.org/>). The cells were cultured in Dulbecco's modified eagle medium (DMEM; Invitrogen, Carlsbad, CA, USA) which consisted of 10% fetal bovine serum (FBS; Invitrogen, USA), 100 U/mL penicillin (Invitrogen, USA) and 100 mg/mL streptomycin (Invitrogen, USA), and maintained in a humidified incubator at 37°C with 5% CO₂.

Preparation and Transfection of miRNA-Microbubble

This experiment was conducted following the procedures as previously described¹¹. For this experiment, microbubbles were available by sonication of an aqueous dispersion consisting of 0.4 mg/ml 1,2-stearoyl-3-trimethylammonium propane with perfluoropropane gas, 1 mg/ml polyethyleneglycol-2000 stearate and 2 mg/ml di-stearoyl phosphatidylcholine (DSPCa). They were obtained from Avanti Polar Lipids Inc. (Alabaster, AL, USA). Then microbubbles were under examination using an inverted microscope (SW380 T, Swift Optical Instruments, Schertz, TX, USA). miR-206 and its mimic control (miR-MC) were added into these microbubbles separately, and they were incubated at 37°C for 30 minutes. HCC cells were then transfected with a mixture of miR-206/miR-MC and microbubbles with Lipofectamine 3000 reagent (Thermo Fisher Scientific, Waltham, MA, USA) for 48 h following the instructions of the producer.

Table 1. Primers of qRT-PCR.

Gene	Primers
miR-206	
Forward	5'-CCTCATAGTCGTATCCAGTGCAA-3'
Reverse	5'-GTATCCAGTGCGTGTCTGG-3'
PPIB	
Forward	5'-GCCCAAAGTCACCGTCAAGG-3'
Reverse	5'-CCACATGCTTGCCATCTAGC-3'
U6	
Forward	5'-CTCGCTTCGGCAGCACATATACT-3'
Reverse	5'-ACGCTTCACGAATTTGCGTGTC-3'
GAPDH	
Forward	5'-GGAGCGAGATCCCTCCAAAAT-3'
Reverse	5'-GGCTGTTGTCATACTTCTCATGG-3'

RNA Isolation and Quantitative Real-Time Polymerase Chain Reaction (qRT-PCR)

Trizol reagent (Invitrogen, Madison, MI, USA) was used to extract total RNA from HCC tissues and cells following the protocols of the producer. Then the extracted RNA was preserved in a -80°C refrigerator. Total RNA concentration was later detected and quantified with a biological spectrometer (Nano Drop 2000, Thermo Fisher, Waltham, MA, USA). CDNA was synthesized from 1 μg of total RNA with a First-strand cDNA Synthesis Kit (E6300 L; New England Biolabs, Ipswich, MA, USA) following the producer's instructions. QRT-PCR experiment was conducted with the SYBR PremixEx Taq II kit (RR820 L, TaKaRa, Shiga, Japan) in the AriaMx real-time PCR System (G8830A, Agilent, Santa Clara, CA, USA). Primer sequences for this experiment are shown in Table 1. GAPDH (for PPIB) and U6 (for miR-206) were used as internal references. Relative gene expressions were quantified using the $2^{-\Delta\Delta\text{CT}}$ calculation method.²⁰

Target Gene Prediction and Dual-Luciferase Reporter Assay

In this experiment, TargetScan 7.2 (www.targetscan.org/) was employed to predict target gene and potential binding sites of PPIB and miR-206, and the prediction was then confirmed by dual-luciferase reporter assay.

Wild-type or mutated PPIB sequences was cloned into the pMirGLO reporter vector (E1330, Promega, Madison, WI, USA) to form the vectors PPIB-wt (sequence: 5'-GGACCCA-CUCCCCUCACAUUCCA-3') and PPIB-mut (sequence: 5'-GGACCCACUCCCCUUUCCAUGA-3'). Then the PPIB-wt and PPIB-mut luciferase reporter plasmids were co-transfected with miR-206 mimic (sequence: 3'-GGUGUGU-GAAGGAAUGUAAGGU-5') or inhibitor (sequence: 3'-ACCUUACAUUCCUUCACACACC-5') into HepG2 cells (5×10^3 cells/well) which were cultured in a 96-well plate using Lipofectamine 3000 reagent (Thermo Fisher Scientific, USA). After 48 h of transfection, the cells were

harvested for luciferase detection in a dual-luciferase reporter assay system (E1910; Promega, Madison, WI, USA) following the manual provided by the producer. Firefly luciferase activity was normalized to *Renilla* luciferase activity.

Western Blot

In our study, western blot was used to detect and measure protein expressions of PPIB and mRNAs related to apoptosis (Bax, Bcl-2), migration, and invasion (E-cadherin, N-cadherin, Snail) as previously described.²¹ Shortly after collecting the cells, the protein was lysed and extracted using RIPA buffer (P0013C, Beyotime, China) and its concentration was then measured using a bicinchoninic acid (BCA) protein kit (P0012 S; Beyotime, China). Thirty μg of protein lysates were subsequently electrophoresed by 12% sodium dodecyl sulfate-polyacrylamide gel electrophoresis (SDS-PAGE; P0012A; Beyotime, China), and then transferred to polyvinylidene fluoride (PVDF) membrane (FFP28; Beyotime, China). After being blocked with 5% non-fat milk for 2 h, the membrane was incubated with the primary antibodies: anti-Bax antibody (rabbit, 1:2000, ab32503, Abcam, Cambridge, UK), anti-Bcl-2 antibody (rabbit, 1:1000, ab59348, Abcam, UK), anti-E-cadherin antibody (rabbit, 1:10000, ab40772, Abcam, UK), anti-N-cadherin antibody (rabbit, 1:1000, ab18203, Abcam, UK), anti-Snail antibody (goat, 1:100, ab53519, Abcam, UK), and anti-GAPDH antibody (mouse, ab8245, 1:1000, Abcam, UK) and anti- β -actin antibody (rabbit, 1:10000, ab181602, Abcam, UK) at 4°C overnight. GAPDH and β -actin were used as internal references. The membrane was subsequently incubated with the secondary horseradish peroxidase (HRP)-conjugated antibodies: goat anti-rabbit IgG H&L (HRP) (goat, 1:2000, ab205718, Abcam, UK), goat anti-mouse IgG H&L (HRP) (goat, ab205719, 1:2000, Abcam) or donkey anti-goat IgG H&L (HRP) (donkey, 1:5000, ab6885, Abcam, UK) at room temperature for 1 h and washed with tris-buffer saline tween (TBST) for 3 times. The protein band collected from the samples was analyzed with an enhanced chemiluminescence (ECL) kit (SW2020; Solarbio, Beijing, China). The gray values of the strips were further gathered and calculated using ImageJ (version 5.0; Bio-Rad, Hercules, CA, USA).

Flow Cytometry

An Annexin V-FITC/propidium iodide (PI) apoptosis kit (catalog number: K101; BioVision, Milpitas, CA, USA) was used for cell apoptosis detection in accordance with the producer's instructions. In short, HepG2 cells were harvested after 48 h of transfection and then washed with PBS twice. Then the cells were treated with Annexin V and propidium iodide (PI) together for 15 min in the dark at room temperature. Cell apoptosis was then analyzed using flow cytometer (APO006; FLISP Serine Protease Detection Kits, Bio-Rad, USA).

Wound Healing Assay

48 hours post transfection, HepG2 cells were seeded in 24-well tissue culture plates at a density of 1×10^4 (cells/ml). A straight wound was then created in the middle of the culture plate with a sterile pipette tip after the cells reached 100% confluence. After being washed with PBS twice to smooth the wound edge and remove floating cells, the cells were then incubated in an incubator (37°C, 5% CO₂). Images of the cells at 0 and 24 h were captured under an inverted optical microscope (SW380 T, Swift Optical Instruments, Schertz, TX, USA). Cell migration was measured using Image-Pro Plus Analysis software (Version 6.0, Media Cybernetics Company, USA).

Transwell Assay

8- μ m-pore transwell chambers (BD Biosciences, San Jose, CA, USA) were placed on 24-well plates with a 50- μ l Matrigel layer coated on Transwell upper chamber (BD Biosciences). Transfected HepG2 cells were then transferred to the upper Transwell chamber at 37 °C with 5% CO₂ to test their invasion ability. After 24 hours, the upper Transwell chamber was washed with PBS several times. Then the non-migrating cells in the upper layer were gently removed with cotton swabs. Subsequently, the Transwell chamber was fixed in a 4% paraformaldehyde solution for 15 min and stained with 0.1% crystal violet for 20 min. Lastly, cell number was counted and photographs were taken using an inverted optical microscope (SW380T, Swift Optical Instruments, USA).

Statistical Analysis

All experiments in our study were conducted more than 3 times independently. Experimental data were expressed as mean \pm standard deviation (SD). Statistical analysis was performed with SPSS 18.0 software (IBM Corporation, Armonk, NY, USA). Statistical significance was analyzed by 1-way ANOVA and student's *t*-test followed by Dunnett's post hoc test. *P*-value < 0.05 indicated a statistically significant difference.

Results

MiR-206 Expression Was Downregulated yet PPIB Expression Was Upregulated in HCC Tissues

In order to determine whether miR-206 plays a regulatory role in the development and progression of HCC, we examined miR-206 expression in 42 pairs of HCC tissues and adjacent normal tissues using qRT-PCR. It was illustrated in Figure 1A that miR-206 expression in HCC tissues (Cancer) was down-regulated compared with adjacent normal tissues (Normal) (*P* < 0.001).

Analysis from gene expression profiling interactive analysis (GEPIA) suggested that PPIB expression was upregulated in HCC tissues (Figure 1B, *P* < 0.05, vs. Normal). In our study, we detected PPIB expression in 42 pairs of HCC tissues and

adjacent normal tissues by qRT-PCR and obtained a similar result. As shown in Figure 1C, PPIB mRNA expression in the Cancer group was upregulated in comparison with the Normal group (*P* < 0.001). These data suggested that MiR-206 expression was downregulated yet PPIB expression was upregulated in human HCC tissues.

PPIB Was the Target Gene of miR-206

With the help of TargetScan 7.2, we successfully predicted the target gene of miR-206, and finally recognized PPIB as the potential target gene of miR-206. Their conserved binding sites, which are listed in Figure 1D., were verified by dual-luciferase reporter assay. The PPIB-wt and PPIB-mut plasmids were co-transfected with miR-206 mimic or inhibitor into HepG2 cells, and meantime, the blank group was established. Our results demonstrated that the luciferase activity in the PPIB-wt-mimic group was reduced yet that in the PPIB-wt-inhibitor group was increased compared with the PPIB-wt-blank group (Figure 1E and F, *P* < 0.001), suggesting that PPIB was the target gene of miR-206.

UTMD-Mediated miR-206 Upregulated miR-206 Expression yet Downregulated PPIB Expression in HepG2 Cells

Cationic microbubble technology has been regarded as an effective method for miRNA delivery.²² To discover the potential effects of UTMD-mediated miR-206 on miR-206 and PPIB expressions in HepG2 cells, we divided HepG2 cells into 6 groups as follows: Mimic control group (MC group): transfected with miR-206 mimic control; Mimic group (M group): transfected with miR-206 mimic; mimic-microbubble + ultrasound group (M-MB + US group): transfected with miR-206 mimic and treated with ultrasonic irradiation and SonoVue microbubbles; mimic control-microbubble + ultrasound group (MC-MB + US group): transfected with miR-206 mimic control and treated with ultrasonic irradiation and SonoVue microbubbles; mimic-microbubble + ultrasound + PPIB group (M-MB + US + PPIB group): on the basis of the M-MB + US group, transfected with PPIB; mimic control-microbubble + ultrasound + PPIB group (MC-MB + US + PPIB group): on the basis of the MC-MB + US group, transfected with PPIB.

Then we measured the transfection rate of miR-206 in HepG2 cells of each group by qRT-PCR. In Figure 2A, it was shown that miR-206 expression in the M group was increased compared with the MC group (*P* < 0.001) yet downregulated compared with the M-MB + US group (*P* < 0.001), while miR-206 expression in the MC-MB + US + PPIB group was lower than that in the M-MB + US + PPIB group (*P* < 0.001), suggesting that UTMD-mediated miR-206 could upregulate miR-206 expressions in HepG2 cells.

Then we detected both the mRNA and protein expressions of PPIB in HepG2 cells of each group by qRT-PCR and western blot, respectively. As Figure 2B-2D showed, after the transfection of PPIB, the mRNA and protein levels of PPIB were

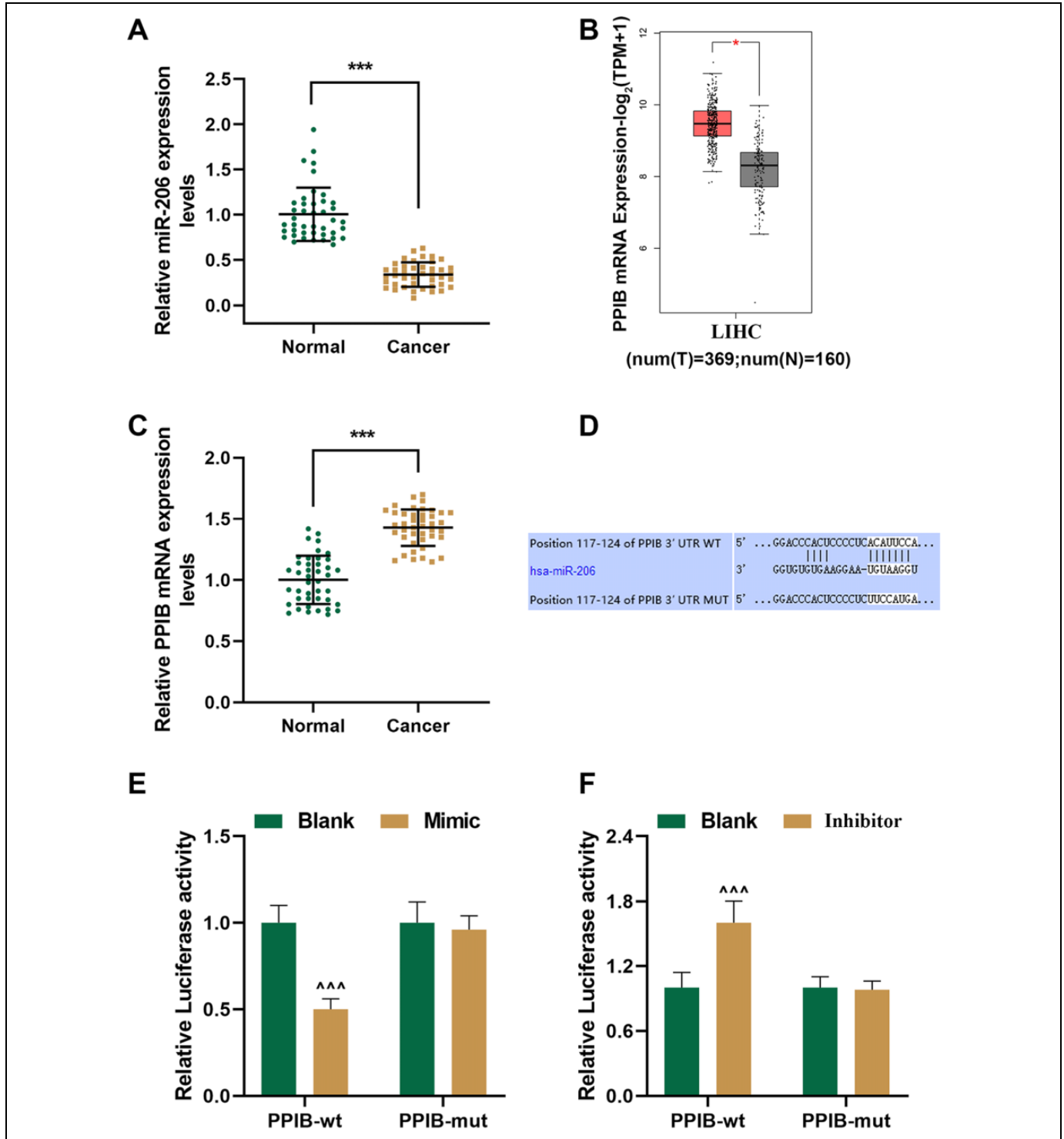


Figure 1. MicroRNA (MiR)-206 expression was downregulated yet peptidyl-prolyl *cis-trans* isomerase B (PPIB) expression was upregulated in human hepatocellular carcinoma (HCC) tissues, and PPIB was the target gene of miR-206. (A) Relative miR-206 expressions in HCC (Cancer) and adjacent normal tissues (Normal) were detected using quantitative real-time polymerase chain reaction (qRT-PCR) ($n = 42$ for each group). U6 was chosen as an internal control. (B) Analysis from gene expression profiling interactive analysis (GEPIA) suggested that PPIB expression was upregulated in liver hepatocellular carcinoma (LIHC) tissues. (T = 369; N = 160) (C) Relative PPIB expressions in Cancer and Normal were detected using qRT-PCR ($n = 42$ for each group). GAPDH was chosen as an internal control. (D) Sequences of the 3'-untranslated regions (3'-UTRs) of wild-type PPIB (PPIB-wt) (top), hsa-miR-206 (middle) and mutated PPIB (PPIB-mut) (bottom) were determined using TargetScan 7.2. (E-F) The results of dual-luciferase reporter assay showed that PPIB was the target gene of miR-206. *** $P < 0.001$, vs. Normal; ^^ $P < 0.001$, vs. Blank.

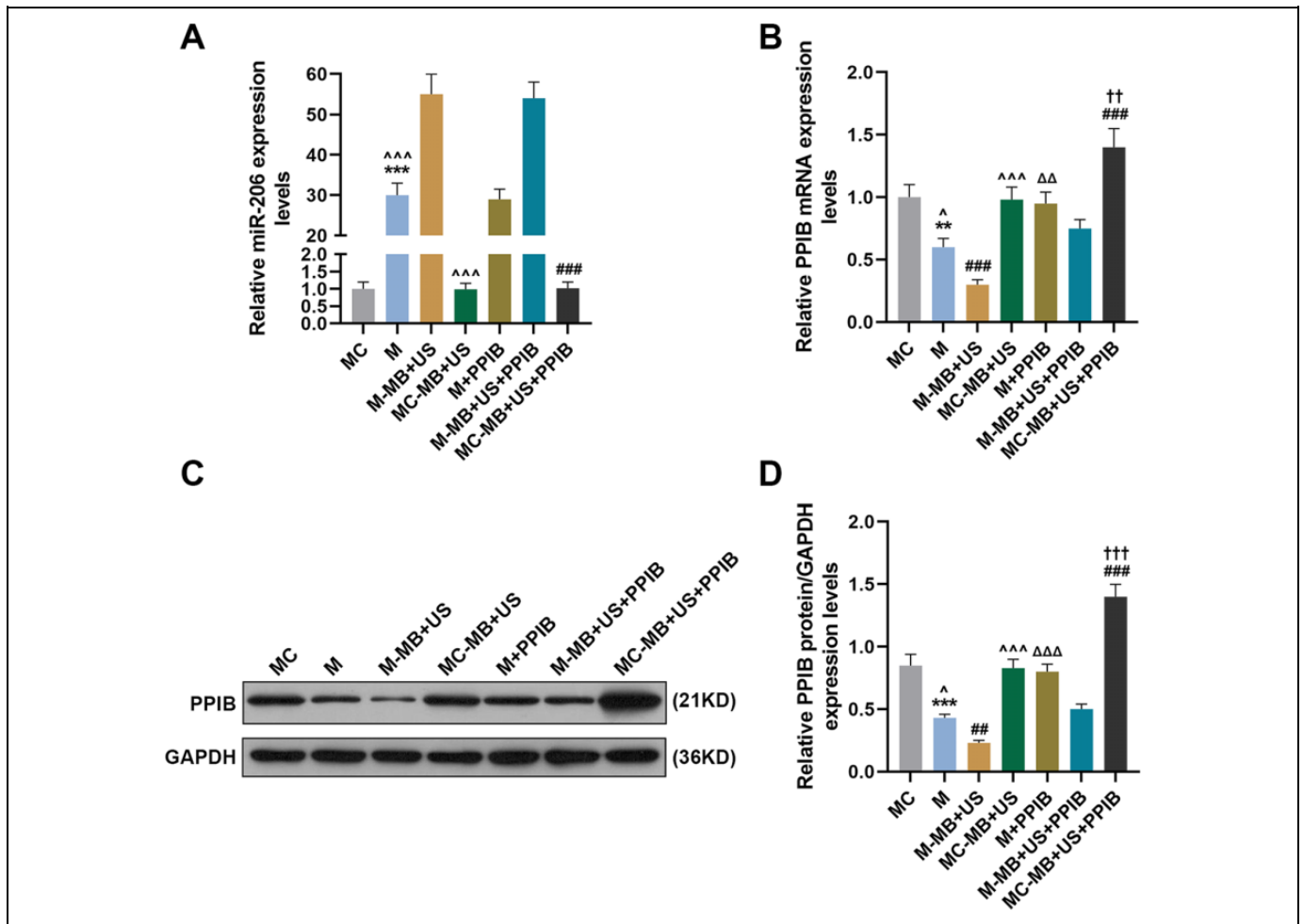


Figure 2. Ultrasound-targeted microbubble destruction (UTMD)-mediated miR-206 could upregulate miR-206 expression yet downregulate PPIB expression in HepG2 cells. **(A)** Relative miR-206 expressions in the MC, M, M-MB + US, MC-MB + US, M + PPIB, M-MB + US + PPIB and MC-MB + US + PPIB groups were measured using qRT-PCR. U6 was chosen as an internal control. **(B)** Relative PPIB mRNA expressions in the MC, M, M-MB + US, MC-MB + US, M + PPIB, M-MB + US + PPIB and MC-MB + US + PPIB groups were measured using qRT-PCR. GAPDH was chosen as an internal control. **(C-D)** Relative PPIB expressions in the MC, M, M-MB + US, MC-MB + US, M + PPIB, M-MB + US + PPIB and MC-MB + US + PPIB groups were measured using Western blot. GAPDH was chosen as an internal control. *** $P < 0.001$, vs. MC; $P < 0.05$, ^^^ $P < 0.001$, vs. M-MB + US; $\Delta\Delta\Delta P < 0.001$, vs. M; ### $P < 0.001$, vs. M-MB + US + PPIB; †† $P < 0.01$, ††† $P < 0.001$, vs. MC-MB + US; MC: miR-206 mimic control; M: miR-206 mimic; MB: microbubble; US: ultrasound.

significantly increased. The mRNA and protein expressions of PPIB in the M group were evidently lower than those in the MC and M + PPIB groups yet higher than those in the M-MB + US group ($P < 0.001$). Also, the mRNA and protein expressions of PPIB in the MC-MB + US group were higher than those in the M-MB + US group yet lower than those in the M-MB + US + PPIB group (Figure 2B-2D, $P < 0.001$). These results demonstrated that UTMD-mediated miR-206 could downregulate PPIB expressions in HepG2 cells.

UTMD-Mediated miR-206 Promoted HepG2 Cells Apoptosis Via Targeting PPIB

We then measured the apoptosis rate of HepG2 cells in each group to discover the potential effects of UTMD-mediated miR-206 on HepG2 cells apoptosis. As Figure 3A and

3B show, HepG2 the apoptosis rate of HepG2 cells in the M group was increased compared with the MC and M + PPIB groups yet lower than that in the M-MB + US group ($P < 0.001$). The overexpression of PPIB could partially reverse the promoting-effects of miR-206 mimic on the cell apoptosis ($P < 0.001$). Besides, it was found that the apoptosis rate in the MC-MB + US group was lower than that of the M-MB + US group ($P < 0.001$). And compared with the M-MB + US + PPIB group, the cell apoptosis rate in the M-MB + US group was upregulated while that in the MC-MB + US + PPIB group was decreased (Figure 3A and 3B, $P < 0.001$).

Since we have discovered that UTMD-mediated miR-206 could promote HepG2 cell apoptosis, its role in regulating apoptosis-related proteins was further investigated. Bax and Bcl-2 have been found to commit a cell to its programmed death,²³ and therefore we detected their expressions in HepG2

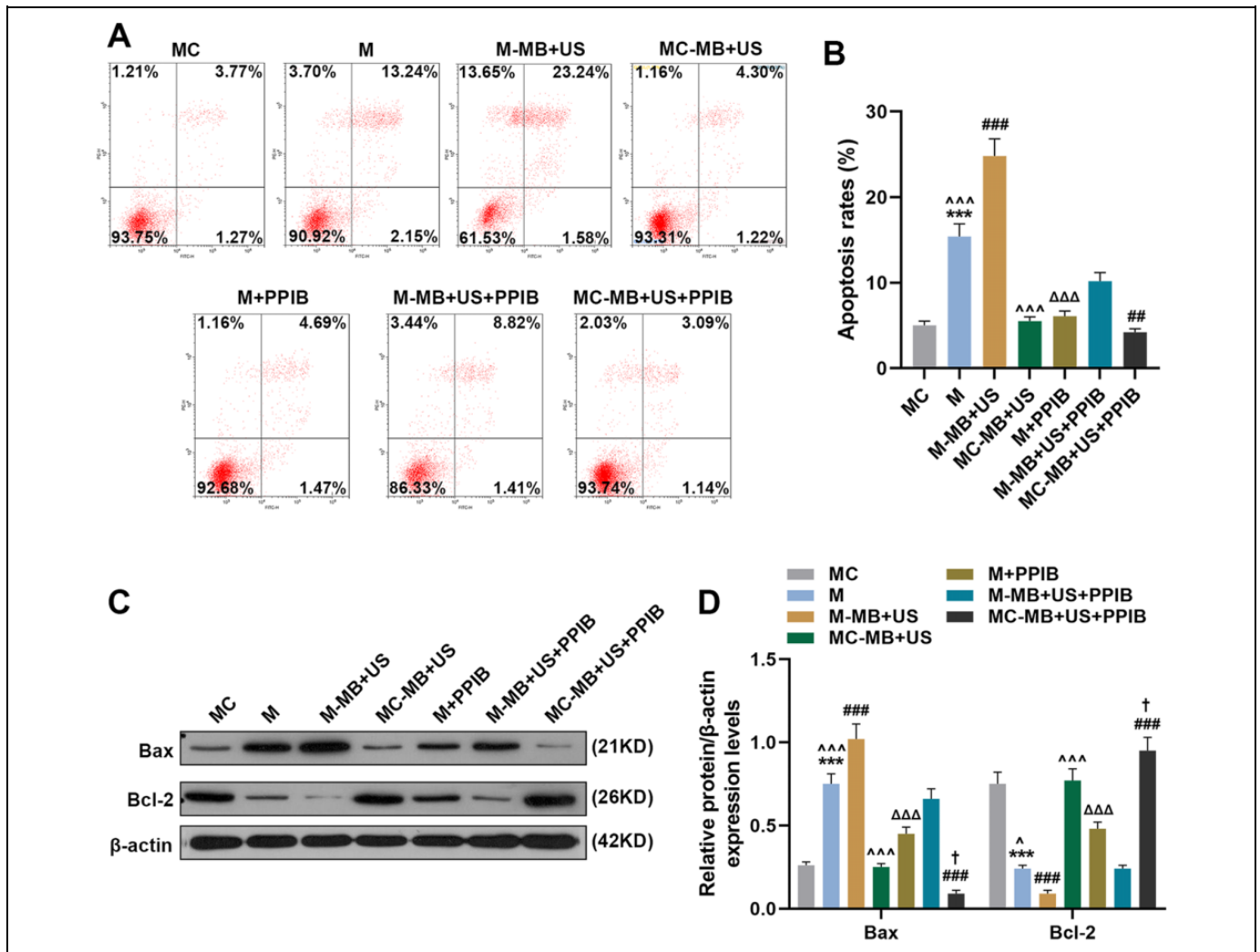


Figure 3. UTMD-mediated miR-206 could promote HepG2 cell apoptosis. **(A-B)** Cell apoptosis rates in the MC, M, M-MB + US, MC-MB + US, M + PPIB, M-MB + US + PPIB and MC-MB + US + PPIB groups were determined by flow cytometry. **(C-D)** Expressions of apoptosis-related proteins Bax, Bcl-2 and β -actin were measured by Western blot. β -actin was chosen as an internal control. *** $P < 0.001$, vs. MC; ^^^ $P < 0.001$, vs. M-MB + US; $\Delta\Delta\Delta P < 0.001$, vs. M; ### $P < 0.001$, vs. M-MB + US + PPIB; † $P < 0.05$, vs. MC-MB + US. Bax: BCL-2-associated X protein; Bcl-2: B-cell lymphoma-2.

cells to further discover the role of miR-206 in cell apoptosis. As exhibited in Figure 3C and 3D, Bax protein expression in the M group was increased compared with the MC group and M + PPIB group yet lower than that in the M-MB + US group ($P < 0.001$). PPIB overexpression showed a strong effects on reversing miR-206-induced the uregularion of Bax and Bcl-2 downregulation ($P < 0.001$). In addition, it was found that Bax protein expression in the MC-MB + US group was lower than that in the M-MB + US group ($P < 0.001$). And compared with M-MB + US + PPIB group, Bax protein expression in M-MB + US group was upregulated while that in the MC-MB + US + PPIB group was decreased (Figure 3C and 3D, $P < 0.001$). However, the protein expression of Bcl-2 in HepG2 cells of each group showed an opposite result (Figure 3C and 3D, $P < 0.001$). These results indicated that UTMD-mediated

miR-206 could promote HepG2 cell apoptosis via targeting PPIB.

UTMD-Mediated miR-206 Inhibited HepG2 Cell Migration and Invasion Via Targeting PPIB

To determine the possible effects of UTMD-mediated miR-206 on HepG2 cell migration and invasion, wound healing assay and Transwell were used to assess the migration and invasion capability of HepG2 cells, respectively. The results of wound healing assay in Figure 4A and 4B exhibited that the relative migration rate in the M group was decreased compared with the MC and M + PPIB groups yet higher than that in the M-MB + US group ($P < 0.001$). In addition, it was found that the relative migration rate in the MC-MB + US group was upregulated in

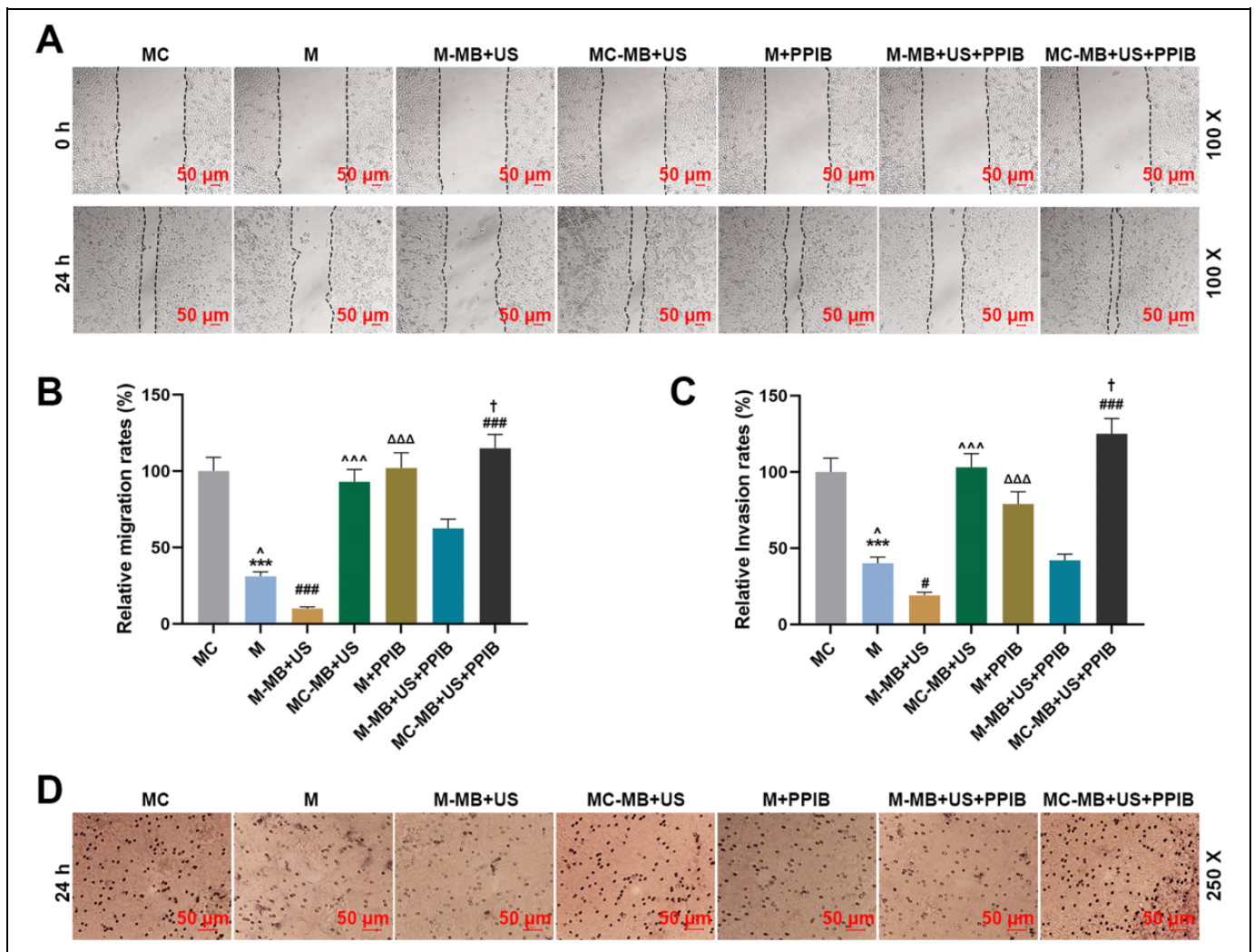


Figure 4. UTMD-mediated miR-206 could inhibit HepG2 cell migration and invasion. **(A-B)** Cell migration rates in the MC, M, M-MB + US, MC-MB + US, M + PPIB, M-MB + US + PPIB and MC-MB + US + PPIB groups at 0 and 24 h were determined by wound healing assay, at 100 × magnification. **(C-D)** Cell invasion rates in the MC, M, M-MB + US, MC-MB + US, M + PPIB, M-MB + US + PPIB and MC-MB + US + PPIB groups at 24 h were determined by Transwell, at 250 × magnification. ^{***} $P < 0.001$, vs. MC; [^] $P < 0.05$, vs. M-MB + US; ^{ΔΔΔ} $P < 0.001$, vs. M; ^{###} $P < 0.001$, vs. M-MB + US + PPIB; [†] $P < 0.05$, vs. MC-MB + US.

comparison to the M-MB + US group (Figure 4A and 4B, $P < 0.001$). And compared with the M-MB + US + PPIB group, the relative migration rate in the M-MB + US group was decreased while that in the MC-MB + US + PPIB group was increased (Figure 4A and 4B, $P < 0.001$).

From the results of Transwell in Figure 4C and 4D, we found that the relative invasion rate in the M group was decreased compared with the MC and M + PPIB groups yet higher than that in the M-MB + US group ($P < 0.001$). In addition, it was found that the relative invasion rate was up-regulated in the MC-MB + US group when compared with the M-MB + US group (Figure 4C and 4D, $P < 0.001$). And compared with the M-MB + US + PPIB group, the relative invasion rate in the M-MB + US group was decreased while that in the MC-MB + US + PPIB group was increased (Figure 4C and 4D, $P < 0.001$). These results were consistent with those

obtained from wound healing assay. Furthermore, after the co-transfection of PPIB, the abilities of cell migration and invasion showed a significant increase, at the same time, the inhibitory effects of miR-206 overexpression on the cell migration and invasion were notably attenuated (Figure 4A and 4B, $P < 0.001$). Taken together, these results indicated that UTMD-mediated miR-206 could inhibit HepG2 cell migration and invasion via targeting PPIB.

UTMD-Mediated miR-206 Regulated the Expressions of EMT-Related Markers in HepG2

Since the EMT process is closely related to cell migration and invasion, in this phase, we measured the expressions of EMT-related markers E-cadherin, N-cadherin, and Snail by Western blot. As shown in Figure 5A-5D, relative E-cadherin/ β -actin

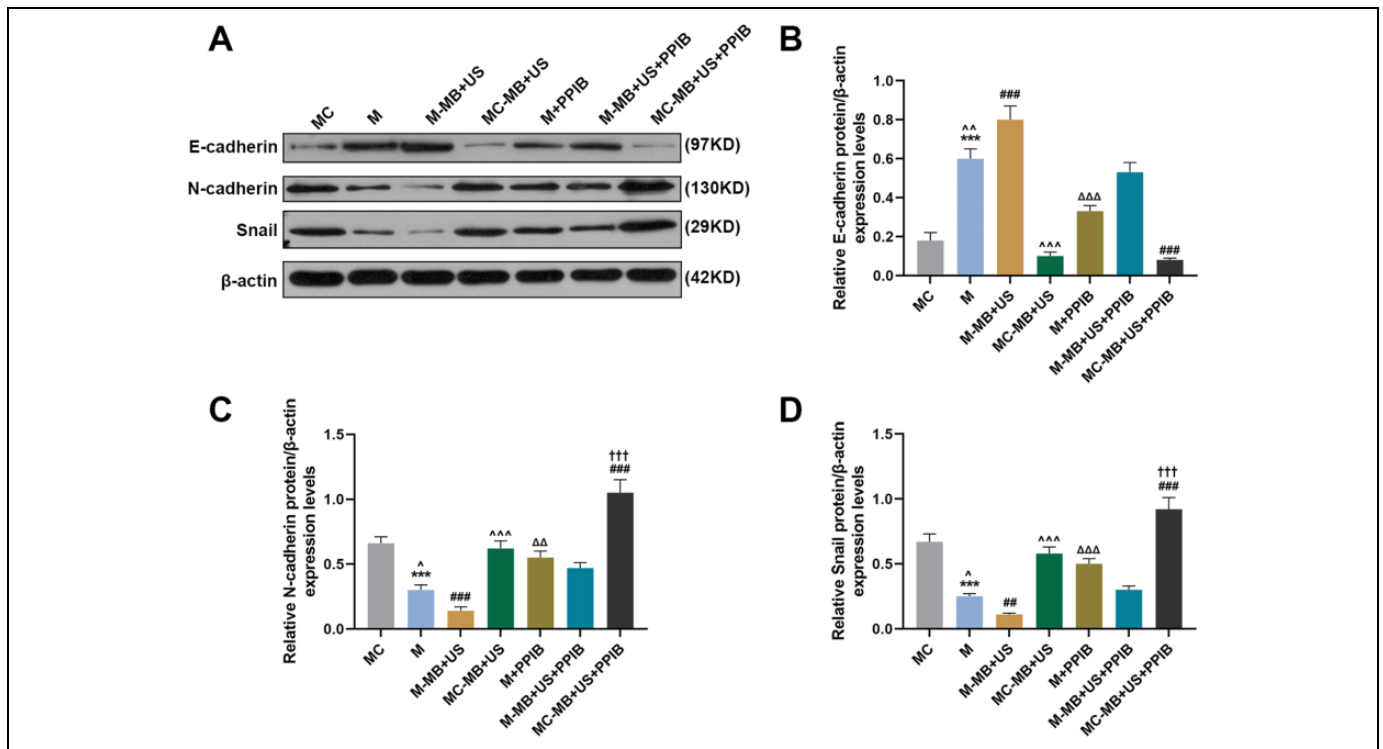


Figure 5. UTMD-mediated miR-206 could inhibit HepG2 cell migration and invasion via regulating the expressions of migration- and invasion-related proteins (E-cadherin, N-cadherin and Snail). **(A-D)** Relative expressions of E-cadherin **(B)**, N-cadherin **(C)**, and Snail **(D)** in the MC, M, M-MB + US, MC-MB + US, M + PPIB, M-MB + US + PPIB, and MC-MB + US + PPIB groups were measured by Western blot. β -actin was chosen as an internal control. $***P < 0.001$, vs. MC; $^{\wedge}P < 0.001$, vs. M-MB + US; $\Delta\Delta\Delta P < 0.001$, vs. M; $###P < 0.001$, vs. M-MB + US + PPIB; $†††P < 0.001$, vs. MC-MB + US.

expression in the M group was increased compared with the MC and M + PPIB groups yet lower than that in the M-MB + US group ($P < 0.001$). In addition, it was found that relative E-cadherin/ β -actin expression in the MC-MB + US group was lower than that in the M-MB + US group (Figure 5A-5D, $P < 0.001$). And compared with the M-MB + US + PPIB group, relative E-cadherin/ β -actin expression in the M-MB + US group was increased while that in MC-MB + US + PPIB group was decreased (Figure 5A-5D, $P < 0.001$). Furthermore, PPIB overexpression showed a strong ability of enhancing the protein levels of N-cadherin and Snail, as well as inhibiting E-cadherin expression (Figure 5A-D, $P < 0.01$). However, an opposite result was found in N-cadherin and Snail protein expressions in HepG2 cells, which therefore proved that UTMD-mediated miR-206 could inhibit HepG2 cell migration and invasion.

Discussion

As more is known about the roles of miRNAs in clinical treatment of human malignancies with mounting evidence,²⁴ miR-206, a highly conserved miRNA in particular, has been found to play a vital role in the development and progression of various cancers, including HepG2.²⁵ Likewise, the present study found that miR-206 had downregulated expression in both HepG2 tissues and cells, and consistent with previous studies, it was found to inhibit HepG2 cell migration and

invasion yet promote apoptosis.²⁵ However, to our best knowledge, we are the first to put forward that UTMD-mediated miR-206 may have better curing effects on inhibiting HepG2 development and progression.

UTMD has been recognized as a novel safe technology with non-invasive properties.²⁶ Specifically, genes attached to microbubbles are injected into blood vessels to circulate inside, and then destroyed by ultrasound insonation at the targeted site.²⁷ Destruction of these bubbles may increase capillary permeability and the generation of holes in cell membranes which released 'payload' that is then incorporated intracellularly.²⁸ In comparison with the traditional viral vector transfection method, the combined method of UTMD and non-viral vectors can more efficiently and safely upregulate the transfection efficiencies of drugs and genes.^{29,30}

In our study, we measured the delivery of UTMD-mediated miR-206 in human HepG2 cells in order to determine and confirm whether the delivery system has a facilitating effect on gene expression in the cells, and examine the changes in cell migration, invasion and apoptosis, as well as elucidate the regulatory mechanisms of miR-206 in HepG2 cells. We found that after transfection with UTMD-mediated miR-206, HepG2 cell migration and invasion were inhibited whereas apoptosis was promoted, accompanied by downregulation of migration- and invasion-related proteins and upregulation of apoptosis-related proteins.

UTMD is a novel method for the delivery of organ-specific genes via sonoporation, which allows the transfer of macromolecule into cells.³¹ It was shown in our present study that in comparison with miR-206, UTMD-mediated miR-206 could enhance the effects of miR-206 on inhibiting the migration and invasion and promoting the apoptosis of HepG2 cells, indicating that UTMD-mediated miRNA delivery may be a possible clinical method for HCC treatment.

The PPIase family consists of broadly expressed enzymes that could accelerate the *cis-trans* proline peptide bonds isomerization.³² PPIB, a member of the PPIase family, has been found to contribute to protein folding,⁸ and its recessive mutations may result in multi-different phenotypes ranging from lethality in the perinatal period to severe deformation in osteogenesis imperfecta.³³ However, its relation with miRNAs was scarcely discussed. In our study, to our best knowledge, we for the first time recognized PPIB as the target gene of miR-206, and found that their expressions were negatively correlated in HCC tissues and cells.

Cancer cell migration and invasion have been found to promote cancer development and progression, in which E-cadherin expression was downregulated yet Snail and N-cadherin expressions were upregulated.³⁴ Studies have shown that miRNAs can inhibit cancer cell migration and invasion via negatively regulating the expression of target mRNAs,³⁵ whereas PPIB has been found to promote non-small cell lung cancer (NSCLC) cell proliferation, metastasis and angiogenesis.³⁶ However, the relation between miR-206 and PPIB in the regulation of HepG2 cell migration and invasion was inadequately discussed. As far as we know, our study was the first to reveal that UTMD-mediated miR-206 could inhibit the migration and invasion of HepG2 cells via targeting PPIB, as well as upregulate E-cadherin expression and downregulate N-cadherin and Snail expressions, which suggests that UTMD-mediated miR-206 may inhibit HepG2 cell migration and invasion via targeting PPIB.

Cell apoptosis has been found to be a defense mechanism against cancer,³⁷ and previous studies have shown that miRNAs are able to promote cancer cell apoptosis by different mechanisms.³⁸ Bcl-2 has been found to be a proto-oncogene with the ability to inhibit cancer cell apoptosis,³⁹ while Bax has been recognized as a pro-apoptosis protein.⁴⁰ A previous study suggested that PPIB could inhibit MPP⁽⁺⁾-induced Bax and Bcl-2 activation.⁴¹ In our study, however, we found that UTMD-mediated miR-206 could promote HepG2 cell apoptosis via targeting PPIB to upregulate Bax expression and downregulate Bcl-2 expression.

However, there are some limitations to our study. In our present study, we only focused on the experiment on HCC cell line HepG2 *in vitro*, but the results were not verified in other HepG2 cell lines. Besides, the efficacy of UTMD-mediated miR-206 in animals needed to be further validated. Therefore, further experiments *in vivo* are required to verify our experimental results.

Taken together, in our study, we successfully transfected miR-206 into HepG2 cells using the UTMD technique, and

found that after transfection, HepG2 cell migration and invasion were inhibited yet cell apoptosis was promoted, which may help researchers gain a better understanding of the effects of miRNA inhibition on cancer progression and development. In addition, we demonstrated that UTMD-mediated miR-206 further enhanced the anticancer efficiency of miR-206 in HepG2 cells, which suggested that UTMD-mediated miR-206 delivery may be used as a potential therapeutic method for HCC treatment.

Declaration of Conflicting Interests

The author(s) declared no potential conflicts of interest with respect to the research, authorship, and/or publication of this article.

Funding

The author(s) received no financial support for the research, authorship, and/or publication of this article.

ORCID iD

Rong Yang  <https://orcid.org/0000-0001-5532-094X>

References

- Schlachterman A, Craft Jr WW, Hilgenfeldt E, Mitra A, Cabrera R. Current and future treatments for hepatocellular carcinoma. *World J Gastroenterol.* 2015;21(28):8478-8491.
- Forner A, Llovet JM, Bruix J. Hepatocellular carcinoma. *Lancet (London, England).* 2012;379(9822):1245-1255.
- Grandhi MS, Kim AK, Ronnekleiv-Kelly SM, Kamel IR, Ghasebeh MA, Pawlik TM. Hepatocellular carcinoma: from diagnosis to treatment. *Surg Oncol.* 2016;25(2):74-85.
- Qadir MI, Rizvi SZ. miRNA in Hepatocellular Carcinoma: pathogenesis and therapeutic approaches. *Crit Rev Eukar Gene.* 2017; 27(4):355-361.
- Krol J, Loedige I, Filipowicz W. The widespread regulation of microRNA biogenesis, function and decay. *Nat Rev Genet.* 2010; 11(9):597-610.
- Xu J, Li J, Zheng TH, Bai L, Liu ZJ. MicroRNAs in the occurrence and development of primary hepatocellular Carcinoma. *Adv Clin Exp Med.* 2016;25(5):971-975.
- Pang C, Huang G, Luo K, et al. miR-206 inhibits the growth of hepatocellular carcinoma cells via targeting CDK9. *Cancer Med.* 2017;6(10):2398-2409.
- Kim G, Kim JY, Choi HS. Peptidyl-Prolyl *cis/trans* isomerase NIMA-interacting 1 as a therapeutic target in hepatocellular carcinoma. *Biol Pharm Bull.* 2015;38(7):975-979.
- Choi TG, Nguyen MN, Kim J, et al. Cyclophilin B induces chemoresistance by degrading wild-type p53 via interaction with MDM2 in colorectal cancer. *J Pathol.* 2018;246(1):115-126.
- Kim Y, Jang M, Lim S, et al. Role of cyclophilin B in tumorigenesis and cisplatin resistance in hepatocellular carcinoma in humans. *Hepatology.* 2011;54(5):1661-1678.
- Qin D, Li H, Xie H. Ultrasoundtargeted microbubble destruction-mediated miR205 enhances cisplatin cytotoxicity in prostate cancer cells. *Molecular medicine reports.* 2018;18(3):3242-3250.
- Tinkov S, Bekeredjian R, Winter G, Coester C. Microbubbles as ultrasound triggered drug carriers. *J Pharm Sci.* 2009;98(6): 1935-1961.

13. Sanguino A, Lopez-Berestein G, Sood AK. Strategies for in vivo siRNA delivery in cancer. *Mini-Rev Med Chem.* 2008;8(3):248-255.
14. Ibsen S, Schutt CE, Esener S. Microbubble-mediated ultrasound therapy: a review of its potential in cancer treatment. *Drug Des. Devel Ther.* 2013;7:375-388.
15. Chen ZY, Liang K, Sheng XJ, et al. Optimization and apoptosis induction by RNAi with UTMD technology in vitro. *Oncol Lett.* 2012;3(5):1030-1036.
16. Chen ZY, Yang F, Lin Y, et al. New development and application of ultrasound targeted microbubble destruction in gene therapy and drug delivery. *Curr Gene Ther.* 2013;13(4):250-274.
17. Guo DP, Li XY, Sun P, et al. Ultrasound-targeted microbubble destruction improves the low density lipoprotein receptor gene expression in HepG2 cells. *Biochem Bioph Res Co.* 2006;343(2):470-474.
18. Kinoshita M, Hynynen K. A novel method for the intracellular delivery of siRNA using microbubble-enhanced focused ultrasound. *Biochem Bioph Res Co.* 2005;335(2):393-399.
19. Kiessling F, Fokong S, Koczera P, Lederle W, Lammers T. Ultrasound microbubbles for molecular diagnosis, therapy, and theranostics. *J Nucl Med Technol.* 2012;53(3):345-348.
20. Livak KJ, Schmittgen TD. Analysis of relative gene expression data using real-time quantitative PCR and the 2(-Delta Delta C(T)) Method. *Methods (San Diego, Calif).* 2001;25(4):402-408.
21. Wang Y, Tai Q, Zhang J, et al. MiRNA-206 inhibits hepatocellular carcinoma cell proliferation and migration but promotes apoptosis by modulating cMET expression. *Acta Bioch Bioph Sin.* 2019;51(3):243-253.
22. Yang D, Gao YH, Tan KB, et al. Inhibition of hepatic fibrosis with artificial microRNA using ultrasound and cationic liposome-bearing microbubbles. *Gene therapy.* 2013;20(12):1140-1148.
23. Edlich F. BCL-2 proteins and apoptosis: recent insights and unknowns. *Biochem Bioph Res Co.* 2018;500(1):26-34.
24. Wang J-Y, Chen L-J. The role of miRNAs in the invasion and metastasis of cervical cancer. *Biosci Rep.* 2019;39(3):BSR20181377.
25. Yang Q, Zhang L, Zhong Y, Lai L, Li X. miR-206 inhibits cell proliferation, invasion, and migration by down-regulating PTP1B in hepatocellular carcinoma. *Biosci Rep.* 2019;39(5):BSR20181823.
26. Zhang L, Sun Z, Ren P, et al. Ultrasound-targeted microbubble destruction (UTMD) assisted delivery of shRNA against PHD2 into H9C2 cells. *PLoS One.* 2015;10(8):e0134629.
27. Ma J, Du LF, Chen M, et al. Drug-loaded nano-microcapsules delivery system mediated by ultrasound-targeted microbubble destruction: a promising therapy method. *Biomed Reports.* 2013;1(4):506-510.
28. Nande R, Howard CM, Claudio PP. Ultrasound-mediated oncolytic virus delivery and uptake for increased therapeutic efficacy: state of art. *Oncolytic virotherapy.* 2015;4:193-205.
29. Chen H, Hwang JH. Ultrasound-targeted microbubble destruction for chemotherapeutic drug delivery to solid tumors. *J Ther Ultrasound.* 2013;1:10.
30. Chen ZY, Lin Y, Yang F, Jiang L, Ge S. Gene therapy for cardiovascular disease mediated by ultrasound and microbubbles. *Cardiovascular Ultrasound.* 2013;11:11.
31. Zheng X, Ji P, Hu J. Sonoporation using microbubbles promotes lipofectamine-mediated siRNA transduction to rat retina. *Bosnian J Basic Med.* 2011;11(3):147-152.
32. Stifani S. The multiple roles of peptidyl prolyl isomerases in brain cancer. *Biomolecules.* 2018;8(4):112.
33. Pyott SM, Schwarze U, Christiansen HE, et al. Mutations in PPIB (cyclophilin B) delay type I procollagen chain association and result in perinatal lethal to moderate osteogenesis imperfecta phenotypes. *Hum Mol Genet.* 2011;20(8):1595-1609.
34. Krakhmal NV, Zavyalova MV, Denisov EV, Vtorushin SV, Perelmuter VM. Cancer invasion: patterns and mechanisms. *Acta Naturae.* 2015;7(2):17-28.
35. Schwarzenbach H. The clinical relevance of circulating, exosomal miRNAs as biomarkers for cancer. *Expert Rev Mol Diagn.* 2015;15(9):1159-1169.
36. Teng M-R, Huang J-A, Zhu Z-T, Li H, Shen J-F, Chen Q. Cyclophilin B promotes cell proliferation, migration, invasion and angiogenesis via regulating the STAT3 pathway in non-small cell lung cancer. *Pathol Res Pract.* 2019;215(6):152417.
37. Labi V, Erlacher M. How cell death shapes cancer. *Cell Death Dis.* 2015;6(3):e1675.
38. Jiang T, Li M, Li Q, et al. MicroRNA-98-5p inhibits cell proliferation and induces cell apoptosis in hepatocellular carcinoma via targeting IGF2BP1. *Oncol Res.* 2017;25(7):1117-1127.
39. Yao C, Cao X, Fu Z, et al. *Boschniackia rossica* polysaccharide triggers laryngeal carcinoma cell apoptosis by regulating expression of Bcl-2, Caspase-3, and P53. *Med Sci Monit.* 2017;23:2059-2064.
40. Xu TB, Li L, Luo XD, Lin H. BMSCs protect against liver injury via suppressing hepatocyte apoptosis and activating TGF-beta1/Bax signaling pathway. *Biomed. Pharmacother.* 2017;96:1395-1402.
41. Oh Y, Jeong K, Kim K, et al. Cyclophilin B protects SH-SY5Y human neuroblastoma cells against MPP(+)-induced neurotoxicity via JNK pathway. *Biochem Bioph Res Co.* 2016;478(3):1396-1402.